CIRP Annals - Manufacturing Technology xxx (2015) xxx–xxx

Contents lists available at ScienceDirect

CIRP Annals - Manufacturing Technology

journal homepage: http://ees.elsevier.com/cirp/default.asp

Metal cutting experiments and modelling for improved determination of chip/tool contact temperature by infrared thermography

Pedro-J. Arrazola (2)[a,*], Patxi Aristimuno [a], Daniel Soler [a], Tom Childs (1)[b]

[a] Faculty of Engineering, Mondragon University, Mondragon 20100, Spain
[b] School of Mechanical Engineering, University of Leeds, LS29JT, UK

ARTICLE INFO

Keywords:
Temperature measurement
Modelling
Cutting tool

ABSTRACT

Temperature measurement in metal cutting at the chip and work contact is of central importance due to temperature dependence of tool wear and surface integrity. Infrared thermography is commonly employed to determine the tool side face temperature in orthogonal cutting but temperature needs to be estimated at the tool chip contact area. This experimental and modelling study of AISI 4140 steel and Ti6Al4V titanium alloy cut respectively by P and K grade cemented carbide tools at practical cutting speeds and feeds shows the relationship between side face and in-contact temperature, for the more certain use of the infra-red thermography method.

1. Introduction

How to measure temperatures in metal cutting at the chip and work contact with the cutting tool continues to receive attention because of the central importance of temperature to the linked problems of tool wear and cut surface integrity [1,2]. One direct method is the tool/work thermocouple technique though it is much criticised for being responsive only to average contact temperature and the uncertainty of its calibration [1]. Another method is infrared thermography. The schematic Fig. 1a shows a camera viewing the side face of a tool used for orthogonal cutting ([3–5], see also [6]). Chip side flow requires that the tool overhangs the work by a width d. A typical value is d = 0.3 mm for uncut chip thickness h = 0.1–0.2 mm. The recorded side face temperature is thus an unknown amount lower than the temperature even at the edge of the contact, let alone lower than that in the contact.

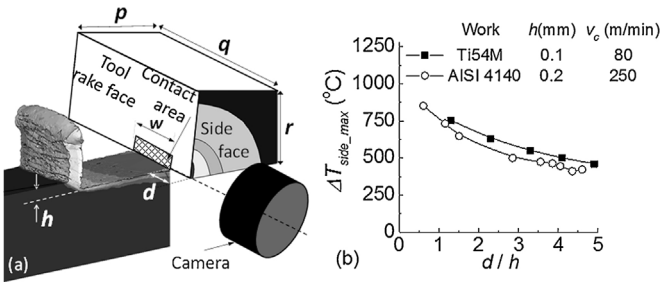

Fig. 1. (a) Schematic view of infrared thermography set up with notation, (b) ΔT_{side_max} dependence on d/h, machining a Ti alloy and a steel [7].

Fig. 1b is a recent result showing ΔT_{side_max}, the maximum side face temperature, reducing the larger is d/h for two typical cases, machining a Ti alloy and a low alloy steel [7]. Measurements also exist for d = 0.3 mm and a range of h and cutting speed v_c. There are published [8–10] comparable measurements by the tool/work thermocouple method. Fig. 2 records results from both methods. Because the h, v_c conditions are not identical, to aid comparison temperatures are partially non-dimensionalised by the specific cutting force F_C^* and h and v_c are combined to the product hv_c.

Fig. 2 shows that for steel the in-contact temperature from the tool/work thermocouple method is significantly higher than the side face temperature from infrared thermography but for Ti alloys the two methods give overlapping results. The hv_c ranges differ between the two groups of alloys due to their different thermal diffusivities.

This paper combines modelling and a modified infrared temperature measurement method to suggest that the difference between the steel and Ti alloy characteristics results from the different tool temperature distributions that occur. The infrared temperature measurement method provides a way directly to view rake face temperatures. Maximum rake face temperature is

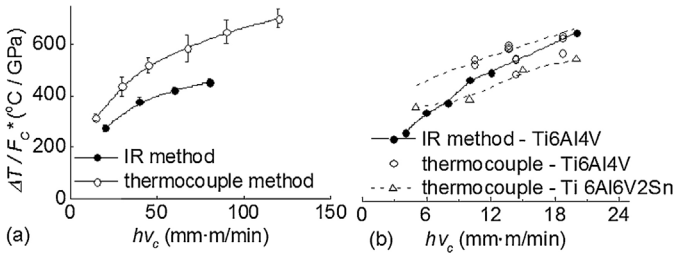

Fig. 2. Comparisons of rake temperature measurements by tool/work thermocouple and infrared thermography methods for (a) AISI 4140, h = 0.2, 0.3 mm; v_c = 50–400 m/min; (b) Ti alloys, h = 0.1–0.25 mm, v_c = 40–110 m/min.

* Corresponding author.
E-mail address: pjarrazola@mondragon.edu (P.-J. Arrazola).

http://dx.doi.org/10.1016/j.cirp.2015.04.061
0007-8506/© 2015 CIRP.

measured 120–380 °C higher than at the side face. This is more than predicted in [6] and significant for understanding tool wear.

2. Modelling and simulation strategy and results

The steady state tool temperature distribution when machining with the orthogonal cutting geometry of Fig. 1a is simulated using the commercial software AdvantEdge-3D, to obtain expected side face and rake contact temperatures at different overhangs d.

Two basic issues are addressed. One is that the typical cut time or distance of a simulation is not usually long enough for the steady state to be reached away from the chip/tool contact region. This is overcome here by choosing the tool density ρ and specific heat C to be much lower than in reality (1000 kg/m^3 and 1 J/kg K respectively): the steady state temperature is reached more quickly the lower is ρC; it does not depend on ρC but only on the tool thermal conductivity K_{tool}. The other is that the size of the tool model is much less than in reality. The tool temperature boundary conditions (fixed temperature, adiabatic, or with heat loss) are consequently artificial. This is overcome by simulations with ever increasing tool size (p, q, r dimensions as in Fig. 1a) and with Newton cooling tool surface boundary conditions of varying heat transfer coefficient h_{tc}, until tool contact and overhang temperatures are obtained insensitive to those conditions.

Fig. 3 explains the tool temperature boundary conditions, their effect on the tool temperature distribution, and the criterion for determining a large enough tool. Newton cooling occurs over all tool surfaces (Fig. 3a) except the side face which is adiabatic, to match the condition of dry cutting. As a result the tool heats up until its surfaces are hot enough for the heat flow from the chip to the tool to be dissipated through the surfaces. In the example the tool is small (p, q, r 1.5–2.5 mm) and h_{tc} = 500 W/m^2 K, slightly high for dry cutting. The tool has heated to ≈800 °C to achieve the steady state. Fig. 3b shows mid-plane tool temperatures for this case. As tool size is increased, the far-regions of the tool become cooler and the temperatures as in Fig. 3b change. A large enough tool is one for which the change becomes negligible. The closer is h_{tc} to a realistic size, the more accurate is the result.

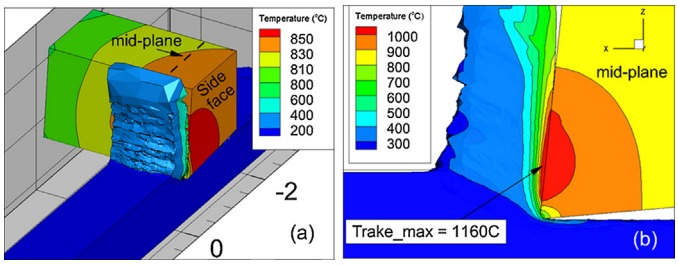

Fig. 3. Example simulation, AISI 4140 cut by P-carbide, h = 0.2 mm, v_c = 250 m/min; w, p, q, r (mm, see Fig. 1) = 1.5, 2.5, 1.5: (a) general view of temperature contours, (b) detail of contact mid-plane section.

2.1. Simulation conditions and outputs

Simulations are performed for AISI 4140 and Ti6Al4V machined by P- and K-carbide tools. Eq. (1) is the flow stress for AISI 4140 up to 900 °C. Above that, flow stress reduces linearly to zero at the AISI 4140's melting point. Eq. (1) is validated experimentally in [8]. Eq. (2) for Ti6Al4V combines a flow stress law (2a) with a plastic failure strain law (2b). It leads to saw-tooth chips though it is not claimed that it does so in a physically realistic manner.

$$\bar{\sigma}\,(\mathrm{MPa}) = 990\left(1+\frac{\bar{\varepsilon}}{0.0094}\right)^{0.029}(1+\dot{\bar{\varepsilon}})^{0.022}(1-6.7.10^{-4}T+3.7.10^{-7}T^2) \quad (1)$$

$$\bar{\sigma}\,(\mathrm{MPa}) = 895\left(1+\frac{\bar{\varepsilon}}{0.076}\right)^{0.19}\left(1+\frac{\dot{\bar{\varepsilon}}}{0.01}\right)^{0.037}(1-6.06.10^{-4}\mathrm{T}) \quad (2a)$$

$$\int_0^{\bar{\varepsilon}_f}\frac{d\bar{\varepsilon}}{0.4\exp[1.5(p/\bar{\sigma})]} = 1.0 \quad (2b)$$

Work thermal conductivity and diffusivity for AISI 4140 are 39 W/m K and 8.7 mm^2/s; and for Ti6Al4V are 6 W/m K and 2.5 mm^2/s. Tool thermal conductivities are 50 W/m K (P-carbide) and 100 W/m K (K-carbide).

Simulations are carried out for h = 0.1, 0.2 mm, v_c = 75, 250 m/min for AISI 4140 and 40, 80 m/min for Ti6Al4V, and for w = 1, 2 mm, to match the conditions of Fig. 2. Tool rake angle γ = 6°. As well as temperature distributions, cutting and thrust forces F_C and F_T are outputs from the simulations.

2.2. Tool size and h_{tc} dependence of tool temperature fields

The simulations' predictions of how tool temperatures stabilise with increasing tool size for different input values of h_{tc} and different machining conditions are summarised in Figs. 4–6.

For machining AISI 4140, with h = 0.1 mm, v_c = 250 m/min (Fig. 4), mid-plane temperature contours do not alter with increasing tool size once a tool size (mm) of (p, q, r) = (5, 4, 5) is reached in the case that h_{tc} = 5000 W/m^2 K (Fig. 4a) but (20, 5, 20) is needed when h_{tc} = 200 W/m^2 K (Fig. 4b). The temperature contours for both these cases are similarly shaped. The main difference between them is that for h_{tc} = 200 W/m^2 K, tool temperatures are 25–50 °C higher than for h_{tc} = 5000 W/m^2 K.

This difference is insignificant compared to changing h and v_c. The stabilised contours for h = 0.2 mm, v_c = 250 m/min, and h = 0.1 mm, v_c = 75 m/min are seen in Fig. 5a and b. As hv_c reduces

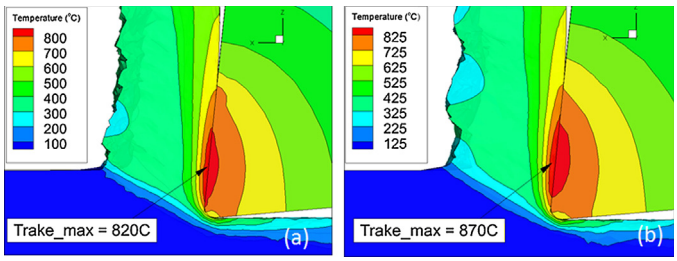

Fig. 4. AISI 4140 cut by P-carbide, h = 0.1 mm, v_c = 250 m/min: h_{tc} (W/m^2 K) and (p, q, r mm) (a) 5000 and (5, 4, 5), (b) 200 and (20, 5, 20).

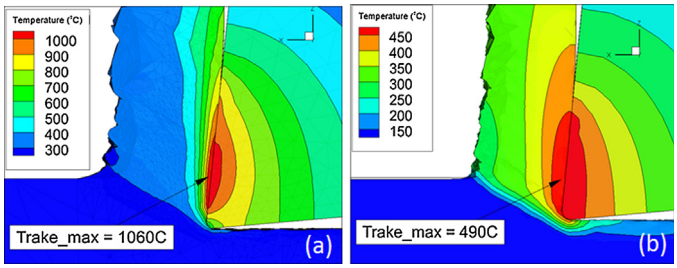

Fig. 5. AISI 4140 cut by P-carbide, h_{tc} (W/m^2 K) and (p, q, r mm) 5000 and, (5, 4, 5): (a) h = 0.2 mm, v_c = 250 m/min; (b) h = 0.1 mm, v_c = 75 m/min.

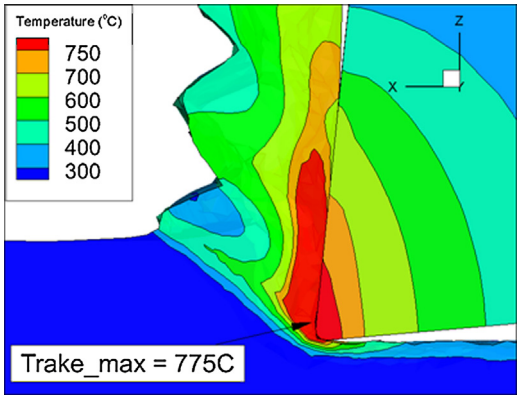

Fig. 6. Ti6Al4V cut by K-carbide: h = 0.2 mm, v_c = 40 m/min, h_{tc} (W/m^2 K) and (p, q, r mm) 5000 and (5, 4, 5).

Please cite this article in press as: Arrazola P-J, et al. Metal cutting experiments and modelling for improved determination of chip/tool contact temperature by infrared thermography. CIRP Annals - Manufacturing Technology (2015), http://dx.doi.org/10.1016/j.cirp.2015.04.061